JOURNAL OF CATALYSIS 133, 515–526 (1992)

Influence of Adsorbed CH_3O on CO Desorption from Ni/Al_2O_3

RAYMOND L. FLESNER AND JOHN L. FALCONER

Department of Chemical Engineering, University of Colorado, Boulder, Colorado 80309-0424

Received June 24, 1991

The desorption rate of CO from the Ni surface of a 5.1% Ni/Al_2O_3 catalyst was significantly increased by the presence of CH_3O on the support. The CH_3O was formed by CO and H_2 coadsorption at 385 K. Reverse spillover of CH_3O, as CO desorbed, maintained the Ni surface at a high coverage of CO and H_2. This increased the rate of CO desorption because of the repulsive interactions present between CO molecules on Ni at high coverages and because readsorption on Ni was decreased. These studies show that CH_3O must undergo reverse spillover onto the Ni surface in order to decompose. Decomposition directly on the Al_2O_3 surface does not occur at these temperatures. Carbon isotope labeling and temperature-programmed desorption were used to study this process. For hydrogen isotope labeling, a kinetic isotope effect for CH_3O decomposition indicated that C–H bond breaking or surface diffusion limited CH_3O decomposition. Oxygen isotope labeling showed that the carbon–oxygen bond did not break upon the formation or decomposition of CH_3O.

INTRODUCTION

Temperature-programmed reaction (TPR) of adsorbed CO in flowing H_2 has shown that two distinct methanation sites are present on Ni/Al_2O_3 catalysts (*1–3*). The more reactive sites were shown to be due to hydrogenation of CO adsorbed on Ni, and the less reactive sites were attributed to a CH_3O species adsorbed on the Al_2O_3 support. The CH_3O species formed by a spillover process in which CO first adsorbed on the Ni surface. A H : CO ratio near three during temperature-programmed desorption (TPD), following coadsorption of CO and H_2 at 385 K, indicated that at saturation the majority of the adsorbed CO was present as CH_3O (*4*). In addition, infrared studies have detected a CH_3O species on a Pt/Al_2O_3 catalyst under the same conditions, and the CH_3O hydrogenated to CH_4 at a different rate than CO adsorbed on Pt (*5*). Infrared spectroscopy has also detected a formate species on the Al_2O_3 support of metal catalysts in the presence of H_2 and CO at elevated temperatures (*5–10*), but this was the least reactive species on Pt/Al_2O_3 (*5*). Also, TPD of formic acid adsorbed on Ni/Al_2O_3 (*11*) gave spectra that were quite different from those obtained for coadsorbed CO and H_2. In contrast, TPD of CH_3OH adsorbed on Ni/Al_2O_3 (*12*), Pt/Al_2O_3 (*13*), and Pt/TiO_2 (*14*) gave CO and H_2 spectra that were quite similar to those observed for coadsorbed CO and H_2. Thus, the species adsorbed on Al_2O_3 under the conditions of our experiments is concluded to be CH_3O. Experiments on physical mixtures of Al_2O_3 and supported Ni catalysts showed directly that the CH_3O was adsorbed on the Al_2O_3 surface (*15*).

The CH_3O formed by a spillover process from Ni to Al_2O_3. The reverse process, in which CH_3O transferred from Al_2O_3 back to Ni, where it decomposed, was also observed (*12*). In that study, the rate of reverse spillover was measured by isothermal treatments in He. Gas phase H_2 appeared to inhibit this reverse spillover.

In the present study, the properties of adsorbed CH_3O and its influence on CO desorption from Ni were studied on a 5.1% Ni/Al_2O_3 catalyst. The CH_3O was created by coadsorption of CO and H_2 at 385 K. These studies show that CH_3O undergoes reverse spillover during TPD, and thus CH_3O affected the desorption of CO from

0021-9517/92 $3.00

Ni. Isotope labeling (^{13}C, ^{18}O, D) was used to study adsorbed CH_3O and its reverse spillover.

Some of the objectives of the present study were to determine:

- How CO desorption from Ni changes as CH_3O coverage on Al_2O_3 increases. Glugla *et al.* (*4*) observed that CO desorption from Ni was significantly modified when CH_3O was on the Al_2O_3 support. Carbon monoxide adsorbed on Ni was labeled with ^{13}C to distinguish it from the products of $^{12}CH_3O$ decomposition.
- The rate of CH_3O decomposition as a function of coverage. The coverage was varied by taking advantage of the activated formation of CH_3O.
- Whether CH_3O decomposes on Al_2O_3 or undergoes reverse spillover in order to decompose.
- If the CO bond remains intact when CH_3O forms and decomposes. Adsorption of $C^{18}O$ was used to follow dissociation.
- If a kinetic isotope effect was present when D was substituted for H in CH_3O.

EXPERIMENTAL METHODS

Temperature-programmed desorption (TPD) and reaction (TPR) experiments were carried out on a 5.1% Ni/Al_2O_3 catalyst. The flow and detection system has been described previously (*16, 17*). Briefly, a 100-mg sample of reduced and passivated catalyst was placed in a 1-cm OD tubular quartz downflow reactor, which was heated by a temperature-programmed electric furnace. A 0.5-mm OD, chromel–alumel thermocouple, placed in the center of the catalyst bed, measured catalyst temperature and provided feedback to the temperature programmer. The catalyst was pretreated at 773 K in H_2 flow (100 standard cm^3/min) for 2 h. Carbon monoxide was then adsorbed at 300 or 385 K by injecting 150 μl (STP) pulses of a 10% CO/He mixture into the H_2 carrier gas with a pulse valve. When ^{13}CO or $C^{18}O$ was used, 50 μl (STP) pulses of the pure gas were injected into the H_2 carrier gas. Note that exposure times for ^{13}CO and $C^{18}O$ adsorption cannot be directly related to those for $^{12}C^{16}O$ adsorption because the partial pressures and the pulse volumes are different.

To obtain TPD spectra of coadsorbed CO and H_2, the catalyst was cooled to 300 K after adsorption was complete, and at 300 K the carrier gas was switched to He. The catalyst temperature was then raised at 1 K/s in ambient pressure He flow (115 standard cm^3/min) to 775–825 K. Species leaving the catalyst surface were detected immediately downstream of the reactor by a computer-controlled, UTI quadrupole mass spectrometer. This system allowed the catalyst temperature and multiple mass peaks to be detected simultaneously.

For some TPD experiments, ^{12}CO was adsorbed at 385 K in H_2 flow and ^{13}CO was then adsorbed at 300 K in H_2 flow. Gas-phase CO readily displaces CO adsorbed on Ni at 300 K (*12, 18, 19*), but gas-phase CO does not exchange with adsorbed CH_3O (*12*). Advantage was taken of this displacement to distinguish CO adsorbed on Ni from that present on the support as CH_3O. After some TPD experiments, the catalyst was cooled in He, the carrier flow was switched to H_2, and a TPR experiment was carried out by raising the catalyst temperature at 1 K/s in H_2 flow. The amount of CH_4 formed was measured to determine the amount of surface carbon deposited by CO disproportionation or dissociation.

For some experiments, CO was adsorbed in D_2 flow (80 standard cm^3/min) instead of H_2 flow to form CD_3O. In those cases, Ar carrier gas (100 standard cm^3/min) was used instead of He during TPD so that a D_2 signal at mass 4 could be detected. Mass signals at $2(H_2)$, 3(HD), and $4(D_2)$ were recorded in addition to those for CO, CO_2, and CH_4. Calibrations were done by injecting known volumes of pure gases. The calibration for HD was taken as the average of those for D_2 and H_2.

The 5.1% Ni/Al_2O_3 catalyst was prepared by impregnation to incipient wetness of Kaiser A-201 alumina (220 m^2/g) with aque-

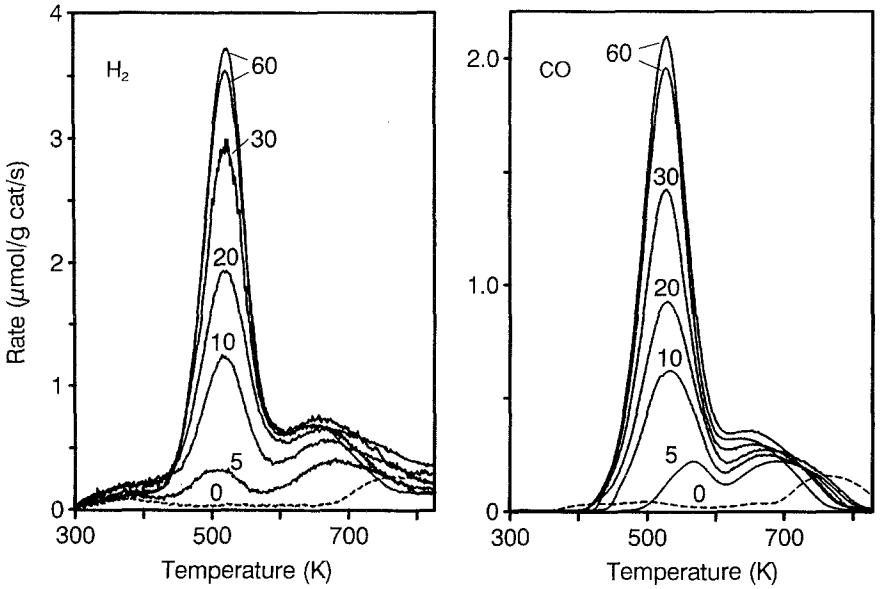

FIG. 1. Hydrogen and CO spectra from TPD of CO adsorbed at 385 K in H_2 flow on a 5% Ni/Al_2O_3 catalyst. Adsorption times are indicated in min.

ous nickel nitrate hydrate. The impregnated Al_2O_3 was dried in vacuum and then directly reduced in H_2 using procedures described previously (*1*). The final reduction temperature was 775 K. The weight loading was measured by atomic absorption. The metal surface area was measured to be 1.4 m^2/g catalyst. The sample was used as a 60–80 mesh powder.

RESULTS

Temperature Programmed Desorption

Initial coverage variation. As reported previously (*4*), when CO and H_2 are coadsorbed at high coverages on Ni/Al_2O_3 catalysts by adsorption at elevated temperatures, their desorption spectra are quite similar. Since previous studies were only done at high exposure, a range of CO exposures in H_2 flow at 385 K were used to obtain the TPD spectra in Figs. 1 and 2. Note that two distinct peaks are observed for desorption. Over the entire range of exposures, the H_2 and CO desorption spectra are quite similar and are significantly different from the desorption spectra obtained when H_2 and CO are adsorbed individually. As shown in Figs. 1 and 2, the spectra are also different from those obtained when H_2 and CO are coadsorbed at 300 K; the zero-min label means CO was adsorbed at 300 K for 10 min in H_2 flow after the catalyst was cooled in H_2 from 775 K, but no adsorption was carried out at 385 K. A 60-min exposure at 385 K is close to saturation coverage on the 5.1% Ni/Al_2O_3 catalyst. The two spectra for 60-min exposure were obtained on different days and demonstrate reproducibility.

At low CO exposures, the majority of the CO and H_2 desorbed above 600 K, but as shown in Fig. 3, for exposures longer than 5 min the amounts in the high-temperature peaks did not increase much. Instead, at higher exposure, most of the CO and H_2 desorbed between 425 and 600 K, and the H_2 and CO spectra had similar shapes. As indicated by the different rate scales in Fig. 1, more H_2 than CO formed. Some differences between the H_2 and CO spectra in Fig. 1 are:

(i) Carbon monoxide desorption was complete by 800 K, but H_2 desorption was not.

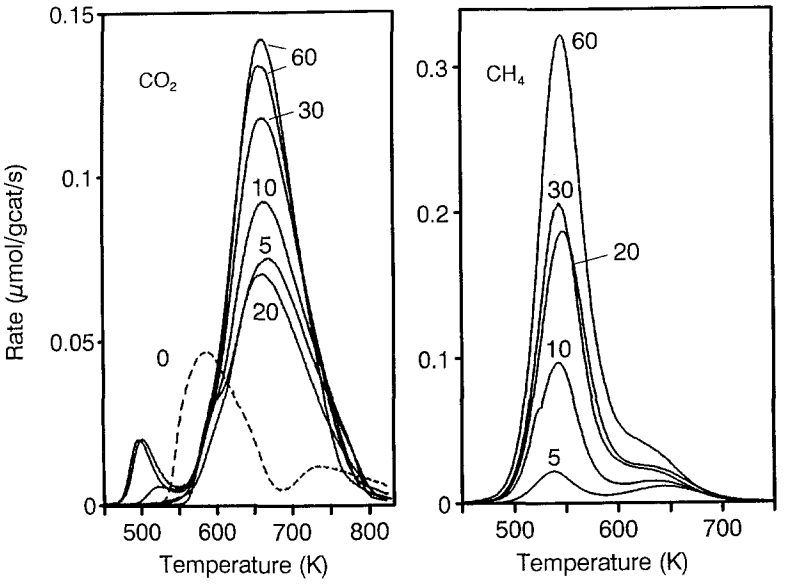

FIG. 2. Carbon dioxide and CH_4 spectra from TPD of CO adsorbed at 385 K in H_2 flow on a 5% Ni/Al_2O_3 catalyst. Adsorption times are indicated in min.

(ii) The CO desorption peak between 425 and 600 K was slightly broader than the H_2 peak (75 versus 70 K half-width).

(iii) A small amount of H_2 desorbed between 300 and 425 K, but CO did not desorb in this range.

(iv) The CO peak temperature was higher than the H_2 peak temperature at each exposure.

With increased coverage, the peak temperature of the low-temperature H_2 peak increased while that of the low-temperature CO peak decreased, as shown in Fig. 4. The CO and H_2 peak temperatures differ by 60 K at low coverage but by only 6 K at high coverage. Most of the change in peak temperature occurred at low coverages. At high coverages, the CO peak was at 527 ± 2 K and the H_2 peak was at 521 ± 1 K. For the high-temperature peaks, the H_2 and CO peak temperatures were almost identical at each coverage, and the peak temperatures decreased as coverage increased.

The H/CO ratio (determined from areas under the curves in Fig. 1) exhibited scatter, but as shown in Fig. 3, the H/CO ratio for exposures greater than 5 min is approximately 3.4 for the low-temperature peaks and 3.2 for the high-temperature peaks. The overlap of the low- and high-temperature peaks at higher exposures made determination of the amounts in each peak less accurate. Repeat experiments for 60-min exposure yielded similar H_2 amounts (353 and 364 μmol/g catalyst) and CO amounts (232 and 208 μmol/g catalyst), but the scatter was amplified in the H : CO ratio (3.0 and 3.4) for the low-temperature peak.

Carbon dioxide and CH_4 also formed during TPD, but their amounts were less than one-tenth that of CO desorption. As shown in Fig. 2, most of the CO_2 desorbed in a peak at 670 K for CO adsorption at 385 K, and the CO_2 amount increased more slowly with exposure than did CO and H_2 (Fig. 3). Most of the CH_4 desorbed in a peak at 546 K. The amount of CH_4 product increased much faster than CO_2 as exposure time increased (Fig. 3). Note that expanded temperature and rate scales (relative to Fig. 1) were used in Fig. 2.

Coadsorption of ^{13}CO and ^{12}CO. As described in the experimental section, ^{13}CO

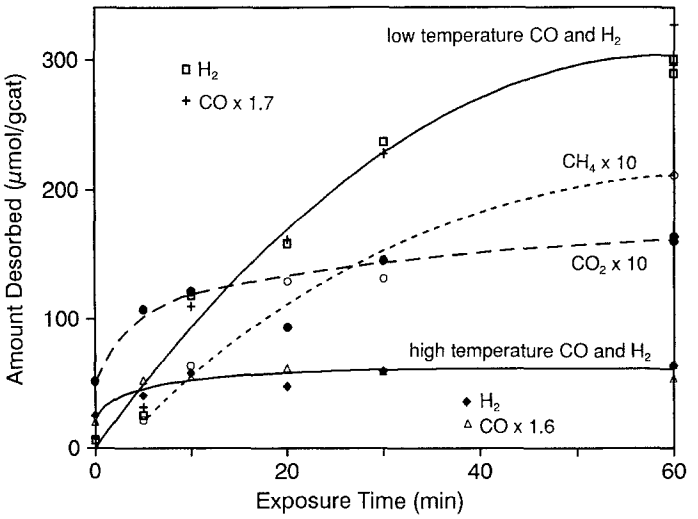

FIG. 3. Hydrogen and CO amounts for the high- and low-temperature TPD peaks and CO_2 and CH_4 total amounts versus CO exposure time. Data are from Figs. 1 and 2. The CO amounts were multiplied by 1.6 (high-temperature peak) and 1.7 (low-temperature peak) so that the H_2 and CO signals for these peaks fell on the same curve.

was adsorbed on Ni and $^{12}CH_3O$ on Al_2O_3 by first adsorbing ^{12}CO in H_2 flow at 385 K. The resulting ^{12}CO on Ni was then displaced by ^{13}CO by exchange at 300 K; the $^{12}CH_3O$ that formed on the Al_2O_3 did not exchange. Figure 5 shows the resulting ^{12}CO and ^{13}CO TPD spectra for several $^{12}CH_3O$ coverages. The most significant result from these experiments is that ^{13}CO desorption from Ni changed significantly as the $^{12}CH_3O$ cover-

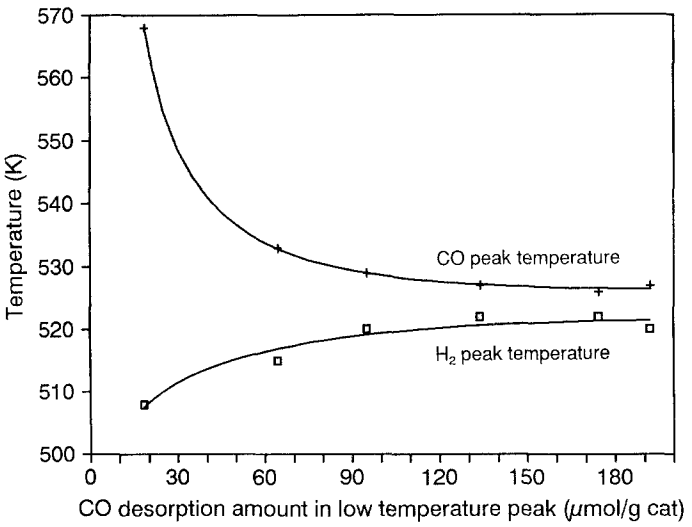

FIG. 4. Hydrogen and CO peak temperatures versus CO quantities in the low-temperature peak for TPD of CO adsorbed in H_2. Data are from Fig. 1.

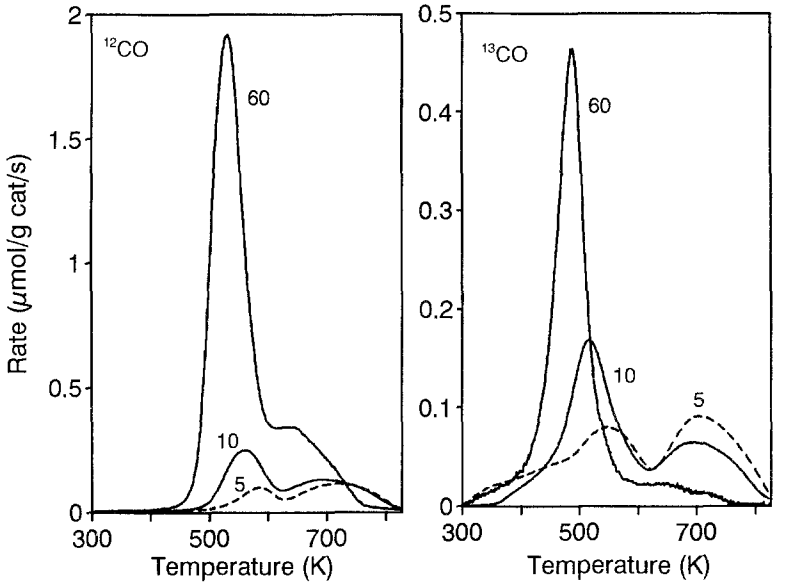

FIG. 5. TPD spectra of ^{12}CO and ^{13}CO following a sequence of ^{12}CO adsorption in H_2 at 385 K and ^{13}CO adsorption in H_2 at 300 K for 10 min. The times (min) are indicated for ^{12}CO adsorption at 385 K.

age on Al_2O_3 increased. The amplitude of the high-temperature ^{13}CO peak decreased significantly, while that of the low-temperature ^{13}CO peak increased. The peak temperature of the low-temperature ^{13}CO peak also decreased from 547 to 487 K as the $^{12}CH_3O$ coverage increased.

The $^{13}CO_2$ amount *decreased* and the $^{12}CO_2$ amount increased as the $^{12}CH_3O$ coverage increased, as shown in Table 1. The carbon-containing species that remained following TPD were removed by reaction with H_2 during TPR. This was carried out immediately after TPD, and the amounts of $^{13}CH_4$ and $^{12}CH_4$ that formed are presented in Table 1. Both $^{13}CH_4$ and $^{12}CH_4$ started forming below 400 K; methanation at this low temperature is indicative of carbon hydrogenation (*16, 20*). As the $^{12}CH_3O$ coverage increased, less carbon deposited on the

TABLE 1

Desorption Quantities for TPD of Coadsorbed ^{12}CO, ^{13}CO, and H_2

^{12}CO Exposure Time[a] (min)	Total amounts desorbed (μmol/g cat)						
	TPD		TPR	TPD			TPR
	^{13}CO	$^{13}CO_2$	$^{13}CH_4$[b]	^{12}CO	$^{12}CO_2$	$^{12}CH_4$	$^{12}CH_4$[b]
0	27	7	4	—	—	—	—
5	30	3	7	33	4	1	3
10	26	2	0	60	6	4	<1
60	34	0	0	173	17	15	0

[a] ^{12}CO was adsorbed at 385 K in H_2 flow, and then the catalyst was exposed to ^{13}CO for 10 min at 300 K.
[b] Methane formed from TPR of surface carbon that remained after TPD.

Ni surface during TPD, and for high $^{12}CH_3O$ coverage no ^{13}C deposited from the ^{13}CO adsorbed on Ni.

Both the $^{13}CO_2$ and the $^{13}CH_4$ amounts in Table 1 show that less ^{13}CO dissociated to carbon and oxygen as the $^{12}CH_3O$ coverage increased. The decrease in the amplitude of the ^{13}CO peak near 700 K is also indicative of less ^{13}CO dissociation, since this peak has been attributed to recombination of carbon and oxygen (*21*). The total amount of ^{13}C leaving the surface (as ^{13}CO and $^{13}CO_2$ during TPD and $^{13}CH_4$ during TPR) was approximately constant at 34 ± 6 μmol/g catalyst, independent of the $^{12}CH_3O$ coverage. Since ^{13}CO was only adsorbed on Ni, the ^{13}CO coverage was not expected to change as the $^{12}CH_3O$ coverage changed. For 5 min of ^{12}CO exposure the ^{13}CO and ^{12}CO peak temperatures (low-temperature peaks) were 547 and 588, respectively. For 60 min of ^{12}CO exposure they both decreased, to 487 and 529 K, respectively. The ^{13}CO desorption also started at much lower temperatures (300–350 K) than ^{12}CO desorption (425–475 K) for all coverages. The sum of the ^{12}CO and ^{13}CO signals in Fig. 5 yield the same spectra as the corresponding ^{12}CO spectra in Fig. 1. The H_2 spectra that were recorded during the experiments of Fig. 5 were also the same as those in Fig. 1.

$C^{18}O$ adsorption. To follow the pathway of oxygen atoms in adsorbed CO and CH_3O, $C^{18}O$ was adsorbed and TPD experiments were carried out at several $CH_3^{18}O$ coverages. Figure 6a shows the TPD spectra for $C^{18}O$ adsorption at 300 K in H_2 flow. As observed in Fig. 1, CO and H_2 desorbed over the entire temperature range. Below 600 K, 59% of the desorbing CO was $C^{18}O$, but above 600 K only 14% of the CO was $C^{18}O$. Most (91%) of the CO_2 was $C^{16}O_2$, and no $^{18}O_2$ was detected. Thus, though the adsorbed $C^{18}O$ was 97% labeled with ^{18}O, 73% of oxygen in the desorbed products was ^{16}O. These spectra are similar to those observed previously for Ni/Al_2O_3 (*22, 23*) and Ni/TiO_2 (*24*). Carbon monoxide adsorbed on Ni dissociates at elevated temperatures, and the resulting oxygen can apparently readily exchange with ^{16}O from the support. The CO_2 that forms as a result of disproportionation can also exchange oxygen with the support.

Figure 6b shows TPD spectra for two coverages of $CH_3^{18}O$: 10 min of $C^{18}O$ exposure in H_2 flow at 385 K (dashed lines) and 30 min of $C^{18}O$ exposure in H_2 flow at 385 K (solid lines). Note that in addition to forming $CH_3^{18}O$, $C^{18}O$ was adsorbed on Ni for these experiments. For both experiments, the majority of the $C^{18}O$ below 600 K was $C^{18}O$, but the majority above 600 K was $C^{16}O$, and no $C^{18}O_2$ was detected. A small amount of $C^{18}O^{16}O$ was observed, but for clarity the $C^{18}O^{16}O$ spectra are not presented in Fig. 6b. The percentage of the total CO desorption that was labeled with ^{18}O increased from 49 to 63% as the $C^{18}O$ exposure increased. That is, the majority of $CH_3^{18}O$ yielded $C^{18}O$ upon decomposition. Thus, the CO bond does not appear to break to form CH_3O or when CH_3O decomposes. However, exchange occurs at the higher temperatures. The CO_2 that forms exchanges with Al_2O_3 more readily than does CO.

In a variation of these experiments, $^{12}C^{18}O$ was adsorbed in H_2 flow at 385 K for 10 min and the catalyst was then exposed to $^{13}C^{16}O$ at 300 K for 10 min. That is, $^{12}CH_3^{18}O$ was formed on Al_2O_3 and $^{13}C^{16}O$ was adsorbed on Ni. Figure 7 shows that for this low CH_3O coverage, less than half the CO that results from CH_3O decomposition is labeled with ^{18}O. The $^{13}C^{16}O$ from Ni desorbs at lower temperatures than $^{12}C^{18}O$, and the high-temperature CO (which is shown to be mostly from the $^{12}CH_3^{18}O$ decomposition) is labeled with ^{16}O. Most of the CO_2 is from $^{12}CH_3^{18}O$, but the oxygen in $^{12}C^{18}O_2$ exchanges with the support. Note that some exchange occurred between $^{13}C^{16}O$ and $^{12}CH_3^{18}O$ during TPD to form $^{13}C^{18}O$.

CO and D_2 coadsorption. To determine how much of the H_2 observed during TPD was from H_2 coadsorbed with CO and Ni rather than from CH_3O decomposition, D_2

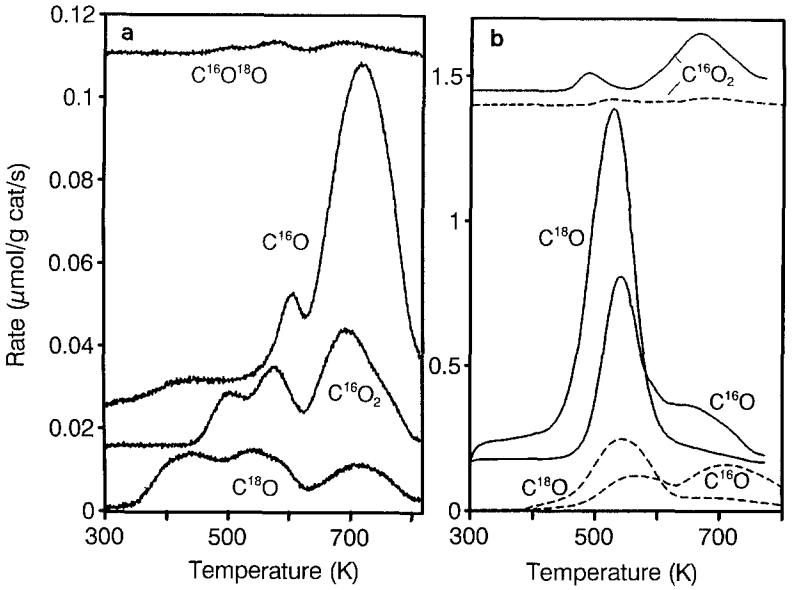

FIG. 6. Carbon monoxide and CO_2 spectra from TPD following (a) $C^{18}O$ adsorption in H_2 at 300 K for 10 min and (b) $C^{18}O$ adsorption in H_2 at 385 K for 10 min (dashed lines) and 30 min (solid lines).

was exchanged with adsorbed H_2 on Ni after CH_3O was formed on Al_2O_3. For this experiment ^{12}CO was adsorbed in H_2 flow at 385 K for 30 min, and the catalyst was then exposed to ^{13}CO in D_2 flow for 10 min at 300 K. During the subsequent TPD in Ar flow (Fig. 8), the H_2 and ^{12}CO from $^{12}CH_3O$ decomposition were similar to those observed previously, but less H_2 desorbed below 425 K. A small amount of D_2 desorbed between 300 and 400 K, and no HD was detected. Thus, the H_2 that desorbs below 400 K in Fig. 1 can be associated with H_2 from Ni, but apparently almost all the H_2 above 400 K is from CH_3O decomposition.

To determine if a kinetic isotope effect exists for methoxy decomposition, $^{12}CD_3O$ was formed by ^{12}CO adsorption in D_2 flow at 385 K (the catalyst was cooled in D_2 flow from 775 K prior to adsorption). The catalyst was then exposed to ^{13}CO in H_2 flow at 300 K to replace ^{12}CO and D_2 adsorbed on Ni. The resulting D_2 and ^{12}CO desorption peaks were similar to the H_2 and ^{12}CO peaks in Fig. 8, but the peak temperatures were higher (7 K for ^{12}CO, 10 K for D_2). That is, CD_3O decomposed more slowly than CH_3O, apparently due to a kinetic isotope effect. No HD or H_2 desorption was detected.

An interesting aspect of this TPD experiment was that ^{13}CO desorption from Ni was also changed when $^{12}CD_3O$ was present instead of $^{12}CH_3O$ on the Al_2O_3. The ^{13}CO peak temperature was 9 K higher than the ^{13}CO peak in Fig. 8. That is, ^{13}CO desorbed more slowly from Ni when CD_3O instead of CH_3O was on the Al_2O_3.

DISCUSSION

In a study on Pd/La_2O_3–SiO_2 catalysts, Guo *et al.* (*25*) concluded that surface migration of adspecies was important in TPD performance. Similar to our observations, they showed that in the presence of adsorbed $^{13}CH_3OH$, the desorption peak temperature of ^{12}CO decreased by 100–150 K. They related the enhancement of ^{12}CO desorption to the decomposition of $^{13}CH_3OH$, which transferred from the support to the Pd. They stated that the interaction of ^{12}CO and ^{13}CO (that formed from $^{13}CH_3OH$ decomposition) caused the lowering of the desorption tem-

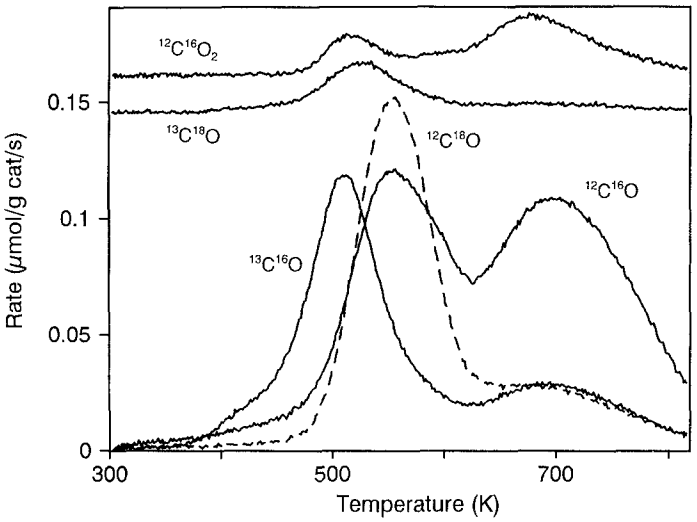

FIG. 7. Carbon monoxide and CO_2 spectra from TPD following $^{12}C^{18}O$ adsorption in H_2 at 385 K for 10 min and subsequent adsorption of $^{13}C^{16}O$ in H_2 at 300 K for 10 min.

perature. They referred to this interaction as a dynamic ensemble mechanism in the desorption of CO at high surface coverage. A similar phenomena was reported by Tamaru and co-workers (*26–28*), who observed that isotopically labeled, gas-phase CO displaced adsorbed CO from polycrystalline surfaces in UHV. They referred to this process as adsorption-assisted desorption, and this is the same process employed in our experiments when adsorbed ^{12}CO on Ni was exchanged by gas-phase ^{13}CO at 300 K. Similarly, ultrahigh vacuum studies by Gland *et al.* (*29–32*) on single-crystal metal

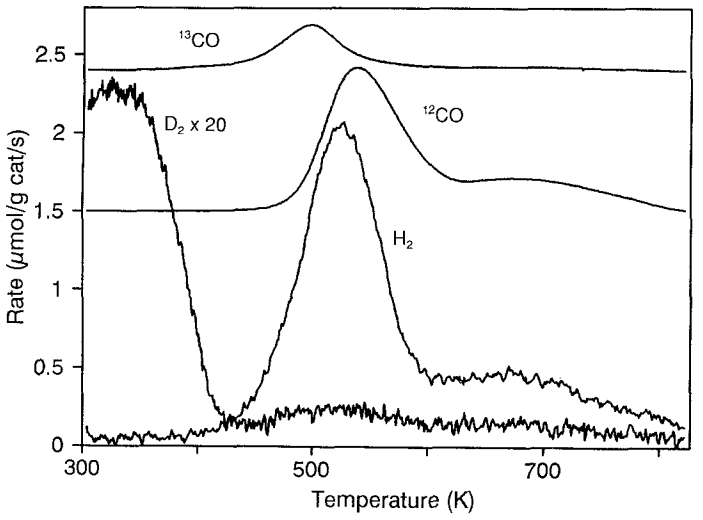

FIG. 8. Hydrogen, D_2, and CO TPD spectra following ^{12}CO adsorption in H_2 at 385 K for 30 min and subsequent adsorption of ^{13}CO in D_2 at 300 K for 10 min.

surfaces showed that gas-phase H_2 caused adsorbed CO to desorb at much lower temperatures than observed in the absence of gas-phase species.

The phenomena observed in these three sets of studies appear to be the same, and Gland *et al.* explained this phenomena as due to repulsive interactions between adsorbed species. In their studies, adsorbed H atoms, in equilibrium with gas-phase H_2, created a higher effective coverage than that due to CO alone preadsorbed on Ni. Thus, the CO desorbed from Ni as if a higher CO coverage was present. As coverage increases, CO is more weakly adsorbed (*18, 33–35*), and they measured a desorption energy of 33 kJ/mol versus 126 kJ/mol for low coverage. The lowering of the desorption energy caused CO to desorb at a lower temperature than in the absence of H_2.

In our TPD studies, the $^{12}CH_3O$ species behaves in the same manner as gas phase H_2 in Gland *et al.*'s studies and gas phase CO in Tamaru *et al.*'s studies. The $^{12}CH_3O$ creates a higher coverage of ^{12}CO and H_2. Thus, as ^{13}CO desorbs from Ni, $^{12}CH_3O$ spills over from Al_2O_3 onto the Ni and maintains a high surface coverage so that ^{13}CO continues to desorb at low temperatures. The ^{12}CO also desorbs at lower temperatures as the $^{12}CH_3O$ coverage increases. Thus, ^{13}CO desorption from Ni depends dramatically on $^{12}CH_3O$ coverage, as shown in Fig. 5.

In addition to repulsive interactions between adsorbed CO, and the CO and H_2 from CH_3O decomposition on the Ni surface of a Ni/Al_2O_3 catalyst, a second effect may also lower the desorption temperature of CO from Ni. During TPD, molecules desorb and then subsequently readsorb as they move through the catalyst bed. When the surface coverage of CO on Ni is maintained high because of reverse spillover, adsorption sites are not available for CO readsorption and thus CO leaves the catalyst bed more rapidly. Both effects are probably responsible for the significant decrease in CO peak temperature as the CH_3O coverage increased.

As desorption decreased the CO coverage at higher temperature during TPD, the remaining CO was more strongly bound to Ni, and because of readsorption some CO remained on the Ni surface to sufficiently high temperature to dissociate and form CO_2 and carbon. Dissociation (or disproportionation) is observed for ^{13}CO adsorbed on the Ni surface alone, but as the $^{12}CH_3O$ coverage increased less $^{13}CO_2$ formed during TPD and less ^{13}C was deposited on the surface (Table 1). At high $^{12}CH_3O$ coverages, no ^{13}CO dissociated and thus no $^{13}CO_2$ was detected. When most of the $^{12}CH_3O$ had decomposed and the ^{12}CO coverage on Ni was low, then readsorption kept ^{12}CO on the surface to higher temperature so that some ^{12}CO dissociated and was responsible for the ^{12}CO peak above 600 K.

Figure 5 shows clearly that as the coverage of $^{12}CH_3O$ increased (longer ^{12}CO exposure time in H_2 at 385 K), much less ^{13}CO (which is adsorbed on the Ni) desorbed above 600 K. When no $^{12}CH_3O$ was present, the CO desorbs mostly at high temperatures (dashed curve in Fig. 1). That is, as the CH_3O coverage increased, the rate of reverse spillover increased so that the coverage on Ni remained high for a longer time, and thus ^{13}CO desorbed at a lower temperature. Thus less ^{13}CO desorbed above 600 K, and the low-temperature peak shifted to lower temperature. Moreover, the low-temperature ^{12}CO peak also shifted to lower temperature.

The similarity between our results for coadsorbed ^{13}CO and $^{12}CH_3O$ and those by Guo *et al.* (*25*) for coadsorbed ^{12}CO and $^{13}CH_3OH$ are another indication that $^{12}CH_3O$ formed from ^{12}CO and H_2 coadsorption, and that $^{12}CH_3O$ had to undergo reverse spillover onto the Ni surface to decompose. That is, the CH_3O, which was formed on Al_2O_3 by spillover, did not decompose on Al_2O_3 at these temperatures. Indeed CH_3OH only decomposed above 600 K when adsorbed on Al_2O_3 that contained no Ni.

The data in Fig. 5 thus indicate that the CH_3O undergoes reverse spillover starting at 450 K for the high coverages of CH_3O.

The CH_3O apparently forms without a significant fraction of the CO dissociating, since the majority of the $C^{18}O$ that was used to form $CH_3^{18}O$ was observed in the desorbing CO. This also means that the carbon–oxygen bond did not break when CH_3O decomposed.

Another indication that reverse spillover controls the rate of CO desorption was obtained by forming $^{12}CD_3O$. The rate of ^{13}CO desorption from Ni was slower when $^{12}CD_3O$ (rather than $^{12}CH_3O$) was on Al_2O_3 because the spillover/decomposition process of $^{12}CD_3O$ was slower. This meant that the ^{12}CO and D_2 peak temperatures were higher than ^{12}CO and H_2 peak temperatures from $^{12}CH_3O$ decomposition, and *the ^{13}CO peak was also at a higher temperature because it depended on the rate of CH_3O spillover and decomposition.*

At low CH_3O coverages the H_2 peak temperature is lower than that of CO; that is, H_2 desorbs more readily than CO following CH_3O decomposition. Apparently this occurs because H_2 is more weakly bound on Ni than is CO. The more rapid desorption of H_2 occurs only for low CH_3O coverages. At high CH_3O coverages, the peak temperatures of H_2 and CO are similar (Fig. 4). Thus, at low CH_3O coverages CO desorption appears to limit the rate of gas phase CO formation, but at higher coverages spillover or decomposition is limiting.

These studies show that CH_3O adsorbed on Al_2O_3 forms gas phase CO and H_2 by reverse spillover and decomposition on Ni so that the majority of the gas phase CO desorbed from a Ni surface at high coverage. However, this does not necessarily mean that CH_3O is hydrogenated during TPR by first undergoing reverse spillover, because the presence of gas phase H_2 significantly decreases the rate of reverse spillover of CH_3O (*36*). Indeed, CH_4 forms at higher temperature during TPR than CO desorbs during TPD. Moreover, during TPR, all the CO can be removed from the Ni without CH_3O moving back onto the Ni. As shown clearly by interrupted TPR (*2, 12*), the CH_3O remains intact on the Al_2O_3. Apparently H_2 prevents the reverse spillover that readily occurs during TPD.

CONCLUSIONS

A CH_3O species formed on the Al_2O_3 surface of Ni/Al_2O_3 from coadsorbed CO + H_2 by a spillover process. The following conclusions were made about the desorption and decomposition of CH_3O and CO adsorbed on Ni/Al_2O_3:

- CH_3O, adsorbed on Al_2O_3 of Ni/Al_2O_3, decomposes by first undergoing reverse spillover onto the Ni, and the CO and H_2 decomposition products desorb from the Ni surface.
- CO adsorbed on Ni desorbs much more rapidly when CH_3O is adsorbed on the support. The reverse spillover of CH_3O maintains a high surface coverage on Ni so that the CO is essentially desorbing from a surface with high coverage. This results in more weakly bound CO and also minimizes readsorption during TPD.
- The combined process of methoxy decomposition and CO + H_2 desorption exhibits a kinetic isotope effect; apparently, decomposition is limited by CH bond breaking or CH_3O diffusion.
- Methoxy both forms on Al_2O_3 and decomposes with the carbon–oxygen bond intact.
- The combination of TPD and C, H, and O isotope labeling is effective for understanding desorption from supported catalysts.

ACKNOWLEDGMENTS

We gratefully acknowledge support by the National Science Foundation, Grant CBT 86-16494. We are grateful to Dr. Keith B. Kester, Dr. Bishwajit Sen, Mr. Tian Fu Mao, and Mr. Baoshu Chen for many useful discussions, and to Dr. John M. Saber for his experimental assistance.

REFERENCES

1. Kester, K. B., and Falconer, J. L., *J. Catal.* **89,** 380 (1984).
2. Glugla, P. G., Bailey, K. M., and Falconer, J. L., *J. Phys. Chem.* **92,** 4474 (1988).
3. Sen, B., and Falconer, J. L., *J. Catal.* **117,** 404 (1989).

4. Glugla, P. G., Bailey, K. M., and Falconer, J. L., *J. Catal.* **115,** 24 (1989).
5. Robbins, J. L., and Marucchi-Soos, E., *J. Phys. Chem.* **93,** 2885 (1989).
6. Dalla-Betta, R. A., and Shelef, M., *J. Catal.* **48,** 111 (1977).
7. Solymosi, F., Bansagi, T., and Erdohelyi, A., *J. Catal.* **72,** 166 (1981).
8. Palazov, A., Kadinov, G., Bonev, C., and Shopov, D., *J. Catal.* **74,** 44 (1982).
9. Lu, Y., Xue, J., Li, X., Fu, G., and Zhang, D., *Cuihua Xuebao (Chinese J. Catal.)* **6,** 116 (1985).
10. Mirodatos, C., Praliaud, H., and Primet, M., *J. Catal.* **107,** 275 (1987).
11. Strobel, M. A., M. S. Thesis, Univ. of Colorado, Department of Chemical Engineering, 1979.
12. Chen, B., Falconer, J. L., and Chang, L., *J. Catal.* **127,** 732 (1991).
13. Flesner, R. L., and Falconer, J. L., in preparation.
14. Mao, T.-F., and Falconer, J. L., *J. Catal.* **123,** 443 (1990).
15. Sen, B., Falconer, J. L., Mao, T.-F., Xu, M., and Flesner, R. L., *J. Catal.* **126,** 465 (1990).
16. Falconer, J. L., and Schwarz, J. A., *Catal. Rev. Sci. Eng.* **25,** 141 (1983).
17. Schwarz, J. A., and Falconer, J. L., *Catal. Today* **7,** 1 (1990).
18. Yates, J. T., Jr., and Goodman, D. W., *J. Phys. Chem.* **73,** 5371 (1980).
19. Klier, K., Zettlemoyer, A. C., and Leidheiser, H., Jr., *J. Phys. Chem.* **52,** 589 (1970).
20. McCarty, J. G., and Wise, H., *J. Catal.* **57,** 406 (1979).
21. Lee, P.I., Schwarz, J. A., and Heydweiller, J. C., *Chem. Eng. Sci.* **40,** 509 (1985).
22. Bailey, K. M., Ph.D. dissertation, Univ. of Colorado, Department of Chemical Engineering, 1988.
23. Galuszka, J., Chang, J. R., and Amenomiya, Y., *J. Catal.* **68,** 172 (1981).
24. Wilson, K. G., Ph.D. dissertation, Univ. of Colorado, Department of Chemical Engineering, 1987.
25. Guo, X., Xu, Y., Zhai, R., Zhu, K., and Huang, J., *Pure Appl. Chem.* **60,** 1307 (1988).
26. Tamaru, K., Yamada, T., Zhai, R., and Iwasawa, Y., *in,* "Proceedings of the 9th International Congress on Catalysis, Calgary, 1988" (M. J. Phillips and M. Ternan, Eds.), Vol. 3, p. 1006. Chemical Institute of Canada, Ottawa, 1988.
27. Yamada, T., and Tamaru, K., *Surf. Sci.* **138,** L155 (1984).
28. Yamada, T., Onishi, T., and Tamaru, K., *Surf. Sci.* **133,** 533 (1983).
29. Parker, D. H., Fischer, D. A., Colbert, J., Koel, B. E., and Gland, J. L., *Surf. Sci.* **236,** L372 (1990).
30. Gland, J. L., Shen, S., Zaera, F., and Fischer, D. A., *J. Vac. Sci. Technol. A* **6,** 2426 (1988).
31. Shen, S., Zaera, F., Fischer, D. A., and Gland, J. L., *J. Chem. Phys.* **89,** 590 (1988).
32. Parker, D. H., Fischer, D. A., Colbert, J., Koel, B. E., and Gland, J. L., submitted for publication.
33. Tracy, J. L., *J. Chem. Phys.* **56,** 2736 (1972).
34. Falconer, J. L., and Madix, R. J., *Surf. Sci.* **45,** 393 (1975).
35. Koel, B. E., Peebles, D. E., and White, J. M., *Surf. Sci.* **107,** L367 (1981).
36. Sen, B., and Falconer, J. L., *J. Catal.* **125,** 35 (1990).